Investigating the Time Response of an Optical pH Sensor Based on a Polysiloxane-Polyethylene Glycol Composite Material Impregnated with a pH-Responsive Triangulenium Dye

Frankaer, Christian G.; Sorensen, Thomas J.

Published in:
ACS Omega

DOI:
10.1021/acsomega.9b00795

Publication date:
2019

Document version
Publisher's PDF, also known as Version of record

ACS OMEGA

Article

Cite This: ACS Omega 2019, 4, 8381−8389

http://pubs.acs.org/journal/acsodf

Investigating the Time Response of an Optical pH Sensor Based on a Polysiloxane−Polyethylene Glycol Composite Material Impregnated with a pH-Responsive Triangulenium Dye

Christian G. Frankær*,† and Thomas J. Sørensen*,†,‡

†Nano-Science Center & Department of Chemistry, University of Copenhagen, Universitetsparken 5, 2100 Copenhagen, Denmark

‡FRS-systems ApS, Hovedgaden 20, 4621 Gadstrup, Denmark

Supporting Information

ABSTRACT: Determining the time it takes a sensor to report a change in the concentration of its target analyte may appear to be an easy task, but it is not. The dynamic characteristic of a sensor is determined by all components in the sensor system and the hydrodynamics of the sample. Here, the dynamic properties of an optical pH sensor were determined using the IUPAC-recommended activity step method in experimental setups that can determine sensor-limited response times longer than 5 s. In order to do so, experimental setups for the injection and for the dipping method of determining the sensor time response were developed, tested, and shown to be able to determine time-response curves with 1 s time resolution. This time resolution is shown to be sufficient for determining dynamic characterization of this optical pH sensor. The sensor chemistry-limited time-response curves were analyzed using curve fitting. It was found that the optode response time is limited by diffusion of protons within the sensor material when the proton concentration is reduced and limited by diffusion from the bulk to the boundary layer at the optode surface when proton concentration is increased. The latter is dependent on the magnitude of the change in analyte concentration and cannot be reported as a single response time. The investigation of the time response of the optical pH sensor reveals detailed information of the sensor chemistry, but does not yield a single response time of the sensor capable of describing the dynamic sensor characteristics of the optical pH sensor system.

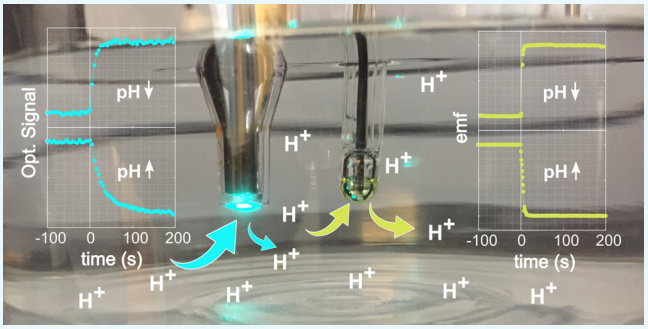

INTRODUCTION

Development of pH sensors started in the beginning of the 20th century when the Danish chemist Sørensen defined pH.[1] He further described two methods to determine pH: the electrometric and the colorimetric.[1] Based on the discovery of the membrane properties of glass, an electrode sensitive to protons was developed.[2−4] A commercial pH meter was launched after 25 years of engineering.[5] The colorimetric pH determination is based on indicator dyes, and the most successful commercialization is indicators immobilized on paper.[6,7] Development of fiber optics, photo diodes, and light-emitting diodes (LEDs) has provided the means for a second implementation of the colorimetric method.[8] During the last 40 years, optical pH sensors have been developed,[9,10] yet only few are commercialized.[11] The challenges for optical sensors are that they require a robust sensor dye that does not photobleach and an inert matrix material in which the sensor dye is robustly immobilized yet still has fast diffusion of protons in and out of the material.[12−15] We have recently reported a new optical pH sensor,[16,17] but as the technology is still emerging, characterization of pH measurements based on the colorimetric method is difficult. This is in stark contrast to pH measurements based on the electrometric method for which standards have been established by the International Union of Pure and Applied Chemistry (IUPAC).[18−20]

When developing new sensors, the dynamic characteristics must be the first to be determined. This is the natural order, as the dynamic characteristics are fundamental to all static characteristics.[21−23] The most important dynamic characteristic is the response of the sensor to an input change, often given as the response time. While standard procedures exist for electrodes,[19,24,25] analogue methods for optodes seem to be nonexistent. We recently discussed the dynamic characterization of optical sensors.[23] Here, we benchmark the response of a pH optode against a commercial pH electrode.[17,23] We recently described our optimized sensor chemistry for determining pH,[17] with pH responsive diazaoxa-triangulenium (DAOTA) dye covalently linked in an ORMOSIL matrix.[16,17,26−28] The change in the fluorescence intensity of the responsive DAOTA emitter is converted into an optical sensor

Received: March 22, 2019
Accepted: April 30, 2019
Published: May 10, 2019

DOI: 10.1021/acsomega.9b00795
ACS Omega 2019, 4, 8381−8389

signal with reference to the emission from a nonresponsive dye.

Addressing and reading the sensor chemistry is done using custom-built hardware that reports both the sensor signal and full emission spectra.[17] Here, only the sensor signal is used to investigate the time-response of an optical pH sensor.

The response of chemical sensors can be limited by all parts of the sensor system, see Figure 1A.[16,17,23,29−31] If all hardware components are fast, the response is determined by the sensor chemistry or by the mass transport of the target analyte in the sensor chemistry. Minimizing the influence of mass transport requires development of an experimental method that enables a change in the target analyte activity at the sensor that is as instantaneous as physically possible, or at least significantly faster than the sensor response itself. To probe the hydrodynamic parameters of the setup, time-response curves recorded with fast-responding commercial pH electrodes were used. With a setup with a fast analyte change and a hardware that enables rapid sampling, the contribution of the sensor chemistry to the time-response can be investigated.[19]

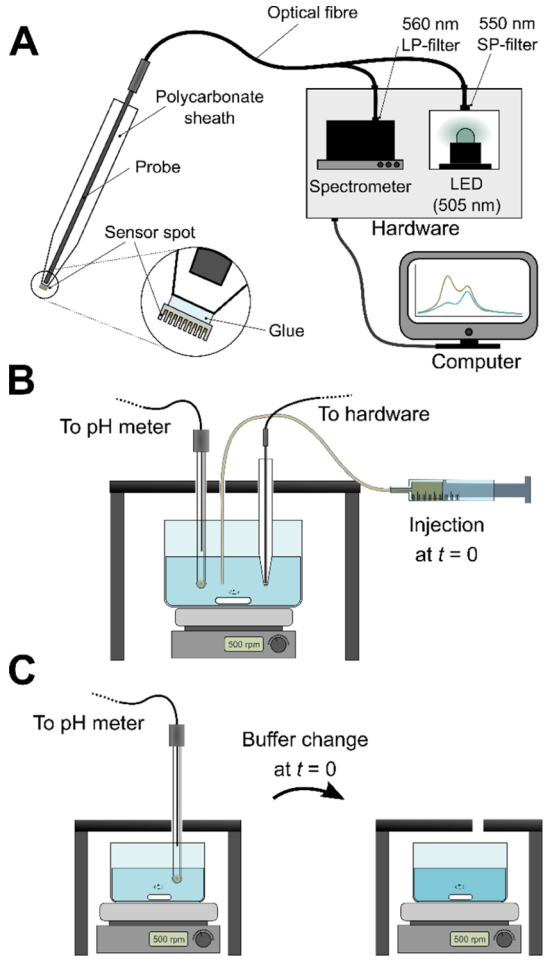

Figure 1. A) Outline of the sensor setup consisting of an optical sensor spot (optode) immobilized in front of an optical probe, fibre optical connectors, hardware encasing a fibre-spectrometer detector, and an LED light source. (B,C) Experimental setup for recording time-response data using the activity step method. (B) The injection method where electrode and optode responses can be recorded simultaneously. (C) The dipping method (here shown with an electrode).

Figure 1 shows the two methods developed for investigating the sensor response.[19,24,32,33] The injection method, shown in Figure 1B, alters the composition of a single solution,[32] while the dipping method, shown in Figure 1C, takes the sensor from one solution to a second.[33] In either method, the sensor responds to an induced activity step change.[19,23] Here, both methods are used to compare the response properties of an optical pH sensor with those of commercial pH electrodes. Using a single magnitude of the activity step, the limiting hydrodynamic conditions were determined. Using the ideal hydrodynamic conditions, the sensor chemistry-limited time response was determined with a resolution of 1 s and setup defined response time determination limits of 5 s (dipping method) and 20 s (injection method).

By investigating the influence of the magnitude of the activity step on the time-response of the optical sensor, the limiting transport processes were identified. For pH electrodes, the previously reported response mechanism was confirmed that is response limited by diffusion from the bulk solution to the electrode surface through a stagnant film.[23] The data showed that the response of the pH optode is limited by two different forms of transport depending on the direction of the activity step. For increasing pH, diffusion within the matrix material is the response limiting process. While for decreasing pH, diffusion from the bulk solution to the optode surface is the limiting process. The results demonstrate the need for a systematic approach when determining response times of chemosensors and clearly indicate which parameters can be optimized when engineering a faster sensor response.

RESULTS AND DISCUSSION

Determination of dynamic sensor properties requires careful design of the experimental method. The workflow used to optimize the experimental setup was recently discussed in great detail.[23] Robust determination of time-response curves is a prerequisite for investigating dynamic sensor characteristics determined by the sensor chemistry.[19,34] In the following, the experimental parameters are investigated to ensure that the response-limiting component of the chemosensors is the sensor chemistry.

Response Curve Analysis. For optical chemosensors, the first important parameter to consider is the activity step used to determine the time-response curve.[23] The pH optode has an operational range of 3 pH units centered at its characteristic pK_a-value of the responsive dye which in this case is 6.1. For setup development, an activity step of 2 pH units (i.e. a 100-fold change in $[H^+]$) centered at the pK_a-value was chosen. This corresponds to the pH change between 5.1 and 7.1. All response curves were recorded in a 2-(*N*-morpholino)-ethanesulfonic acid (MES) buffer system, which has a pK_a-value of 6.15 resulting in an optimal overlap between the buffer region of high buffer capacity and the operational range of the sensor.

Figure 2 shows representative normalized time-response curves for optodes and electrodes recorded for pH decrease or increase by 2 pH units. The response curves contain error, σ, determined as ∼2.5% for optodes and ∼0.5% for electrodes. Thus, the response times for optodes and electrodes should be determined as t_α with $\alpha < 97.5\%$ and $\alpha < 99.5\%$, respectively.[23] The optical signal output from the optode was determined as the fluorescence intensity ratio between the pH responsive dye and the reference dye,[17] and the signal output from the electrodes is the open circuit potential. Time-response curves

DOI: 10.1021/acsomega.9b00795
ACS Omega 2019, 4, 8381−8389

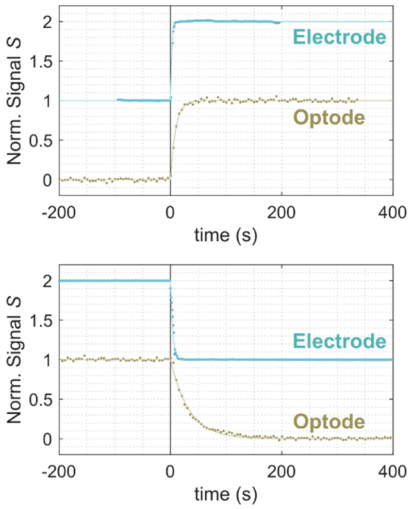

Figure 2. Selected normalized time-response curves for optodes (olive) and electrodes (blue) showing signal outputs, S, as a function of time. Top: pH decrease from 7.1 to 5.1. Bottom: pH increase from 5.1 to 7.1. (·) Experimental data (—) curve fit using eq 1.

are the signal output, S, plotted as a function of time, t.[19,23,35] A first order empirical model was used for curve fitting analysis of the time-response curves using the following equation[23,36]

$$S(t) = \begin{cases} S_0 & \text{for } t < 0 \\ S_\infty - (S_\infty - S_0)\exp(-k\,(t - t_d)) & \text{for } t \geq 0 \end{cases} \quad (1)$$

where S is the sensor signal changing from S_0 to S_∞, and subscripts 0 and ∞ denoting initial and final steady-state signal values. t_d is the delay time, which is defined as the length of time between introduction of the input change of the operator and the first significant effect of the input change seen in the output, thereby including both dead time and lag time, see ref 23. k is the rate constant defined as $1/\tau$, where τ is the time taken to obtain a signal conversion of ∼63%.

For optodes, Figure 2 shows that 90% of the response (t_{90}) has occurred after approx. 20 and 60 s for pH decrease and increase, respectively. Similar t_{90}-values for electrodes are 5 s. As shown in Figure 2, response data were recorded long enough to ensure that the steady-state signal could be determined with high confidence. Each steady-state value was determined at 5 × t_{90}, which corresponds to a signal conversion α of >99.99% using the model described by eq 1.[23]

Prior to curve fitting analysis, all time-response curves were normalized against the steady-state signal output using the following procedure: The baseline was calculated by averaging the data points recorded before the activity step change and the steady-state signal was calculated by averaging all data points recorded after 3 × t_{90}. This corresponds to a signal

Table 1. Response Characteristics of Optical pH Sensors

manufacturer/ reference	short description of pH sensor, and test procedure	quantity &; value	
Presens	pH optode. Well agitated solutions at 37 °C. No specifications on pH jump reported	t_{90}	<120 s
Finesse	pH optode. Agitated solutions. Activity jump or temperature not reported	t_{90}	<60 s
Polestar	pH optode. No description of method	t_{90}	<40 s
Ocean Optics	Optode integrated in a cuvette. No description of method	t_{90}	∼10 s
37	absorption intensity of Congo Red immobilized in a TEOS matrix and deposited on a PMMA fibre. Response tested by immersion of a probe into standard buffers ranging with a pH change from 8 to 5 (a), or pH change from 5 to 8 (b)	t_{90}	(a) t_{90} ≈2 s, (b) t_{90} ≈ 4 min
38	fluorescence lifetime of ruthenium complexes immobilized in hydrogels and deposited on polyester substrates. pH change from 6.5 to 9 (a) and from 9 to 6.5 (b)	t_9, t_{99}	(a) t_{90} ≈ 7−10 s, (b) t_{90} ≈ 10−25 s
39	ratiometric fluorescence intensity of HPTS immobilized in a PDMS/APTES/TEOS matrix on an optical fibre. Response tested by immersion of probe into 100 mM Tris buffers. pH change from 2.5 to 8.3	t_{90}	t_{90} = 13 s
40	absorption intensity of phenol red in a TEOS/PhTES matrix and deposited on glass slides. Response tested by immersion of glass slides in cuvettes. pH change from 5 to 10 (a) and pH change from 5 to various pH in the range 8 to 12 (b)	t_{95}	(a) t_{95} ≈ 5−600 s[a], (b) t_{95} ≈ 30 s[b]
41	evanescent wave absorption of bromocresol purple and bromocresol green immobilized in TEOS on silica fibres. pH change from 4 to 11 (a), and from 11 to 4 (b)	?	(a) ∼5 s, (b) ∼30 s
42	absorption variation of swelled TEOS/TMOS without dyes deposited on a silica fibre. Absorption varies with pH. pH change from 2.0 to 10.4 and back	t_{90}	t_{90} ≈ 1−5 min
43	ratiometric fluorescence intensity of mercurochrome immobilized in a TMOS/MTMOS matrix. Optode was made by packing fragmented sol−gel particles in a flow cell. Tested in the pH range 3 to 8	t_{90}	t_{90} ≈ 3−4 min
44	combined pH/DO/temperature sensor. The pH sensor is based on fluorescence life time of HPTS immobilized in a PMMA/ aminoethylacrylamide matrix on an optical fibre, Tested in buffers with a pH change from 9 to 4 (a), and 4 to 9 (b)	t_{95}	(a) t_{95} ≈ 2 min, (b) t_{95} ≈ 3 min
45	ratiometric fluorescence intensity of chlorophenyliminopropenylaniline and the reference dye Macrolexfluorescence yellow 10 GN immobilized in a PVC/bis(2-ethylhexyl)phthalate matrix on a polyethylene terephthalate substrate. pH change from 7 to 9 and back	t_{90}	t_{90} ≈ 60 s
46	fluorescence intensity of Ru complexes immobilized in a TEOS/PhTES matrix on an optical fibre. Tested by immersion of the probe into buffers in the pH range of 2.0−8.1	?	30 s
47,48	ratiometric excitation intensity of HPTS immobilized in GPTMS/ETES on glass. Tested in a flow cell with a pH change from 5 to 7 and back	t_{90}	t_{90} = 12 s
49	absorption intensity of methyl red and bromocresol green immobilized in a TEOS/GPTMS matrix on glass slides. Response tested by immersion in cuvettes with 0.1 M HCl then buffer with a pH of 8.06 (a) and back (b)	t_{95}	(a) t_{95} ≈ 20 s, (b) t_{95} ≈ 1 s
50	fluorescence intensity of aminofluorescein immobilized in a TMOS/PhTES matrix, on glass slides. Response tested in 20 mM phosphate buffer with a pH change from 4.7 to 8.3 (a) and 8.3 to 4.7 (b)	t_{95}	(a) t_{95} ≈ 90 s, (b) t_{95} ≈ 120 s
51	fluorescence intensity of fluorescein immobilized in a PVA/TMOS matrix on glass. Tested in a flow cell with a pH change from 3 to 9 (a) and 9 to 3 (b)	t_{95}	(a) t_{95} ≈ 6 min, (b) t_{95} ≈ 2.5 min

[a]Depending on sol−gel composition. [b]Faster from pH 5 to 12, than from pH 5 to 8.

DOI: 10.1021/acsomega.9b00795
ACS Omega 2019, 4, 8381−8389

conversion α of ~99.9% using the model in eq 1. That is, the steady-state signal was evaluated from data sampled beyond 99.9% conversion. In this time interval, any change due to the activity step change will be within the error σ. Note that within the given level of σ, drift was not detected.[23]

The curve fitting analysis using eq 1 is suitable for determining the dynamic properties of the pH optode and the pH electrodes. All time-response curves and corresponding curve fits are included in the Supporting Information.

Influence of Experimental Conditions. Attention to experimental conditions is crucial if useful and reliable time-response curves are to be obtained. Time-response curves from systematic data analysis may reveal the properties of the sensor chemistry. Table 1 highlights this by compiling time-response information from commercial pH optodes and from optical pH sensors reported in the literature. As the experimental conditions in all cases are different—and in most cases only partially described—comparing the reported information is difficult. We may tentatively conclude that the pH optode investigated here has a response time similar to or lower than that of other optical sensors based on fluorescence. However, to compare the performance of the sensor chemistries, more attention must be given to the experimental conditions.

The conditions described in the experimental section are those used for determining the activity step dependence, and these have been carefully optimized. However, both of the IUPAC recommended methods have their limitations: the response time determined by the injection method is limited by the homogenization time and hydrodynamic conditions, which may influence the first part of the time-response curve.[23] But because the position of the electrode/optode remains unchanged, the method is excellent for determining whether a response is instantaneous. When using the dipping method, the data points collected during the period where the electrode/optode is moved between samples interrupt the continuity of the time-response curve, and rejection of these data may be required. Hence, judging whether a response is instantaneous relies on how fast the switch between reservoirs can be performed. Here, this time was 2−3 s. To illustrate possible pitfalls, examples on how the hydrodynamic conditions influence the time-response curves must be discussed.

Figure 3 shows time-response curves from pH optodes and pH electrodes following a pH decrease from 7.1 to 5.1 using the injection method. The curves in the center and bottom panel of Figure 3 were recorded at a very slow agitation speed (50 rpm). When injection of acid is carried out far from the optode (i.e. the bottom of the reservoir), delay times of 30−40 s were observed, see Figure 3 bottom panel. When acid is injected in vicinity of the optode/electrode (i.e. in the same depth as the optode/electrode tip), fluctuations in the sample solution result in a signal overshoot, see Figure 3 central panel. Such curves are not suitable for response time analysis and should be avoided. The conclusion is that injection far from the optode/electrode and close to the agitator provides acceptable homogenization of the sample solution before the effect of the activity change is sensed, thereby ensuring monotonous time-response curves suitable for determination of response times.

High speed agitation, however, may also result in inadequate time-response curves, as seen in the top panel of Figure 3. Agitation at 900 rpm generates bubbles that lead to unstable hydrodynamic conditions. The effect is most prominent for the optode, where bubbles build up on the surface of the optode

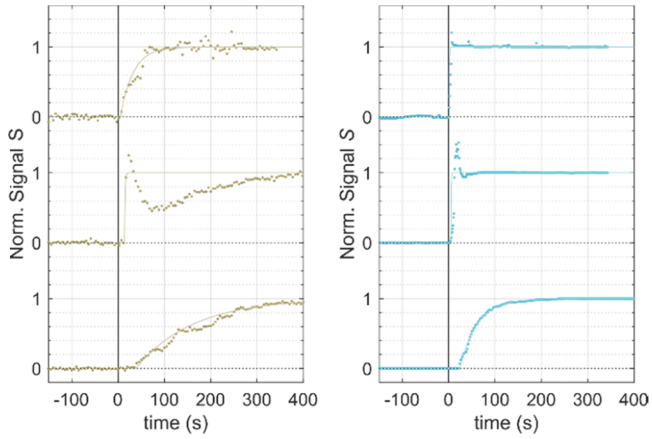

Figure 3. Normalized time-response curves for optodes (left; olive) and electrodes (right; blue) recorded under different hydrodynamic conditions for pH decrease from 7.1 to 5.1. Bottom: delay time observed when using the injection method with a very low agitation speed (50 rpm), and injection far from the electrode/optode. Center: overshoot when using the injection method with a very low agitation speed (50 rpm) and injection in the proximity of the electrode/optode. Top: increased error when using a high agitation speed (900 rpm) which induces bubbles that disturb the measurement.

disturbing the measurement, but the effect was also observed in the response of the pH electrode, where an increased σ is observed (see the Supporting Information).

Another important parameter to consider when using the injection method is the injection speed relative to the time resolution of the experiment. Figure 4 shows two time-

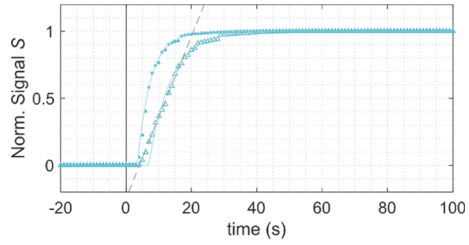

Figure 4. Normalized time-response curves for a glass electrode recorded at a high agitation speed (600 rpm) with a time resolution of 1 s. Injection was performed at two different rates: 20 (▲) and 100 mL/min (●). A linear tangent was fitted to the first part of the time-response curve recorded with 20 mL/min as a guide for the eye.

response curves for a glass pH electrode recorded at a high agitation speed (600 rpm) providing fast homogenization and thereby a fast sensor chemistry-limited response. The hardware has a time resolution of 1 s, and injection was performed at two different rates: 20 and 100 mL/min. Using a volume of 4 mL 1 M HCl, the injections are completed within 12 and 2.4 s, respectively. Figure 4 shows that a response is observed for both rates of injection after a delay time of approx. 5 s, but that the response is markedly slower for injection at 20 mL/min. The time-response is almost linear and is identical to the rate of injection. Careful analysis of the result reveals that the electrode response is fast in this case and the limiting factor is the rate of injection. As the object of study is the sensor and the sensor chemistry of the pH optode in particular, the rate of injection-introduced artefact is a problem, and we must conclude that in the injection method the injection must be completed within a time period shorter than the time

DOI: 10.1021/acsomega.9b00795
ACS Omega 2019, 4, 8381−8389

resolution of the experiment (1 s). Thus, the experimental setup must be optimized for agitation speed, positions of sensors and injection, and speed of injection if reliable time-response curves are to be determined with the injection method.

At agitation speeds <400 rpm, it was observed that time-response curves recorded from electrodes were susceptible to overshoots, as seen in the central panel of Figure 3. Overshoots occurred even if the injection was carried out far from the tip of the electrode. The susceptibility towards an overshoot is a result of the fast electrode response, see Figure 2. Slower responding bulk sensors i.e., the pH optode studied here, are less susceptible to overshoots. Therefore, we investigated the effect of agitation on the time-response curves using different setups for the slower optodes and the fast electrodes.

For a slower optical pH sensor, the injection was carried out in vicinity of the pH optode, see the detailed setup in Supporting Information Figure S1, and time-response curves Figures S2–S4, S9–S11, and S14–S16. A series of time-response curves recorded at different agitation speeds for a pH decrease from 7.1 to 5.1 is shown in Figure 5a. Response times evaluated as t_{90}, are plotted as a function of agitation speed in Figure 5c.

For the fast sensors, fast injection (100 mL/min) was carried out in vicinity of the agitator (see the detailed setup in Supporting Information Figure S1 and time-response curves in Figures S5, S6, S12, S13, S17, S18). A series of time-response curves recorded at different agitation speeds of a pH electrode for a pH decrease from 7.1 to 5.1 are shown in Figure 5b. Response times evaluated as t_{90} are plotted as a function of agitation speed, see Figure 5d.

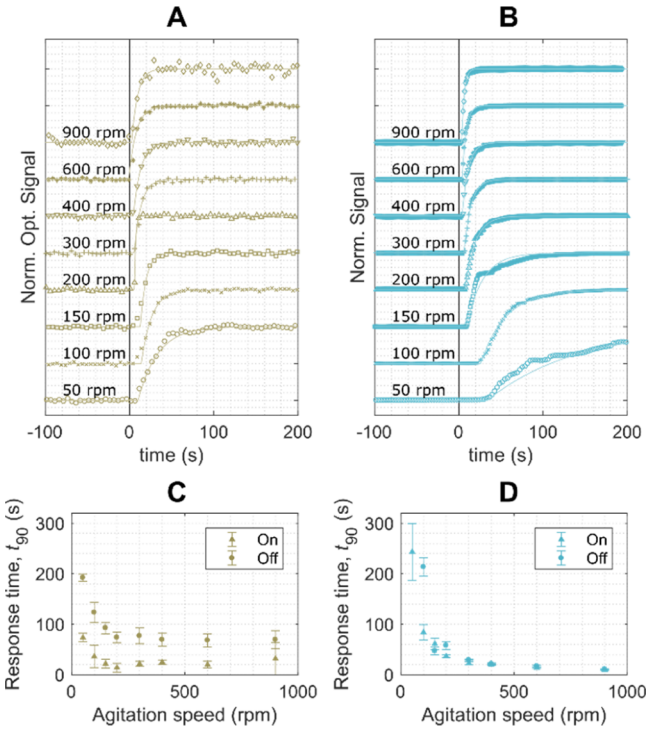

Figure 5. Correlation between response and agitation speed for the pH optode (left; olive) and the pH electrodes (right; blue). (A,B): normalized time-response curves recorded at different agitation speeds for a pH decrease from 7.1 to 5.1. Injection is performed in vicinity of the optode (A), but at the bottom of the reservoir for the electrode (B) to avoid an overshoot. (C,D): response time evaluated as t_{90} plotted against the agitation speed for the pH decrease (on; ▲) and pH increase (off; ●).

In either case, an increase in the response time was observed when decreasing the agitation speed. For the fast electrochemical sensors, a time resolution of 1 s was used. Although the overshoot was avoided by injection close to the agitator, a significant delay time was observed, ∼40 s at 50 rpm. The delay time decreases with increasing agitation speeds and settles at ∼5 s for agitation speeds higher than 200 rpm. A slower colorimetric sensor was investigated with a time resolution of 5 s. Here, the injection close to the agitator resulted in no significant delay time.

The critical setup parameters, agitation speed and the duration and position of the injection, are summarized in Table 2. Within the experimentally determined values, the dynamic sensor properties can be determined from the curve fitting.[23] These are included in Table 2. Using the injection method to induce a pH decrease, both pH optodes and pH electrodes are characterized by a response time of t_{90}∼20 s. However, for a pH increase the optode response is slower, while the electrode response is unchanged. To rationalize this observation, we need to look at the influence of the magnitude of the activity step.

Elucidating Physical Processes Involved in the Response. With the optimized setup, the influence of the size of the activity step magnitude on the response of the sensors was investigated. The response times given as t_{90} were determined by curve fitting analysis using eq 1 (see Figures S9–S18). Figure 6 shows the correlation between t_{90} and the magnitude of the activity step for the two experimental methods. A comparison shows that t_{90}-values determined using the injection method are typically 10–20 s higher than those determined by the dipping method. This is a general trend for both optodes and electrodes, and it is particularly pronounced for high activity steps, where the injection volume is large. As the data analysis takes delay time into account, this indicates the presence of a setup induced time delay of ∼15 s, originating from the mixing process that will be present in any geometry where pH is adjusted by adding acid or base to a stirred solution.

By analyzing the data in Figure 6, we concluded that the setup clearly limits the response time that can be ascribed to the sensor, and that this limiting behavior for each method is reflected directly by the fast responding electrodes. Thus, the sensor related response times that can be determined must be slower than ∼5 s for the dipping and ∼20 s for the injection method. Hence, we can conclude (i) that the activity change experienced by the sensor for each method is completed within 5 and 20 s, respectively, and (ii) that the sensor chemistry-limited response time, t_{90}, is less than 5 s for the electrodes used in this study in both directions of the activity step.

Further characterization of the response of the glass electrodes will require a flow system,[34] analogue to the methods described in references,[52,53] and subsequently a higher data readout frequency (the pH meter used only allows one readout every second).

All response times determined for optodes, given as t_{90}, exceed 5 s. Thus, all time-response curves recorded for optodes using the dipping method are limited by the sensor chemistry. With the injection method, optode response times exceeding 20 s are only observed for activity steps where $\log(a_0/a_\infty) > -1$, meaning that time-response curves recorded using this

DOI: 10.1021/acsomega.9b00795
ACS Omega 2019, 4, 8381−8389

Table 2. Setup Requirements and Response Properties of the Optode and the Electrode Determined by the Injection Method

	optode	electrode
Setup		
agitation speed (rpm)	>300	>300
injection duration (s)	<8	<2.4[a]
Injection position	1 cm below the surface	injection tube
time resolution, t_{res} (s)	5	1
t_{max} (on/off) (s)	>300/> 600	>300/> 300
activity step, a_0/a_∞ (on/off)	100/0.01	100/0.01
Data		
noise, σ	~2.5%	~0.5%
α_{max}	97.5%	99.5%
Curve Fit		
model type	eq 1	eq 1
k (on/off)[b]	0.14 ± 0.04/0.034 ± 0.006	0.17 ± 0.04/0.14 ± 0.05
t_{90}[b]	22 ± 5/71 ± 12	19 ± 4/23 ± 5
t_{95}[b]	27 ± 6/93 ± 15	23 ± 5/28 ± 7
t_{99}[b]		33 ± 7/40 ± 11
delay time, t_d	<7 s	<6 s
goodness of fit, R^2	>0.994	>0.994

[a]Maximal injection rate possible with given equipment. [b]Mean of fitted time-response curves from 3 optodes or 2 electrodes recorded at agitation speeds 300, 400, and 600 rpm.

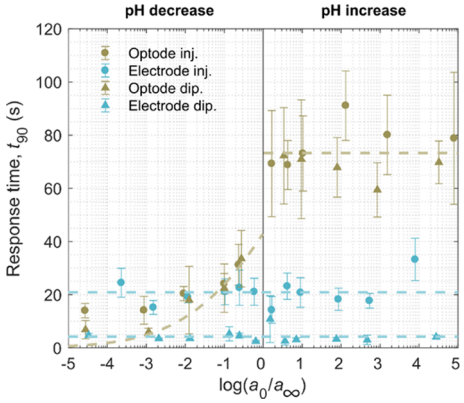

Figure 6. Response time t_{90} for optodes (olive) and electrodes (blue) measured by the injection method (●) and the dipping method (▲), and plotted as a function of the magnitude of the activity step a_0/a_∞.

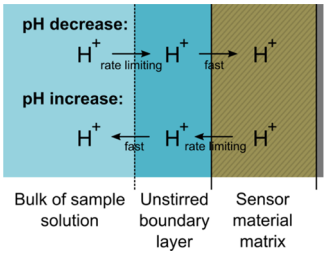

Figure 7. Diffusion routes of protons at the interface between the optode and the sample solution through an unstirred boundary layer. The rate-limiting processes are indicated.

method will contain method-induced contributions when $\log(a_0/a_\infty) \leq -1$, that is, in all experiments where pH is decreased.

For the optodes, the fastest response was observed when pH was decreased (proton activity increased). The response of increased pH was significantly slower (proton activity decreased). This suggests that two different processes, as outlined in Figure 7, control the response.

When the proton activity is increased ($\log(a_0/a_\infty) < 0$), the response time decreases with increasing activity step, indicating a diffusion controlled response. That is, diffusion of protons within the boundary layer covering the optode surface limits the time-response of the optode response. In this case, the driving force is the $[H^+]$-gradient, which is controlled by the activity step size. It was found that the diffusion model described in ref 25 was able to describe all 36 time-response curves for activity steps with increased proton activity (three optodes, each six different activity steps, two methods, see Figures S19–S24) with a single response parameter, k

$$k = \frac{\pi^2 D}{4\delta^2} \quad (2)$$

where D is the mean diffusion coefficient and δ is the thickness of the boundary layer, see the Supporting Information for details. This value was determined, $k = 0.06 \pm 0.01$ s^{-1}. The result is included in Figure 6 (olive dashed; left panel).

When the proton activity is decreased ($\log(a_0/a_\infty) > 0$), the response time was observed to be independent of the activity step size, and diffusion of protons within the organic phase of the optode is controlling the response speed.[54] It was found that the diffusion model described in ref 54 was able to describe all 36 time-response curves for activity steps with decreased proton activity (three optodes, each six different activity steps, two methods, see Figures S19–S24) with a single response parameter, $k = 0.027 \pm 0.006$ s^{-1}. The result is included in Figure 6 (olive dashed; right panel).

Having identified the response limiting processes directly informs how the response time can be minimized. For a rapid response when the pH increases, the thickness of the sensor material film must be reduced, while a rapid response when the pH decreases can be achieved by minimizing the boundary layer thickness. The latter can be achieved by minimizing the surface tension of the sensor matrix, for example, by surface functionalization.

DOI: 10.1021/acsomega.9b00795
ACS Omega 2019, 4, 8381−8389

CONCLUSIONS

The dynamic sensor properties of an optical pH sensor were determined. By recording time-response curves under varying hydrodynamic conditions, an experimental setup was developed and experimental parameters were optimized to ensure that the sensor response is determined by the properties of the sensor chemistry. The experimental setup developed here is able to determine sensor limited response times higher than 20 s for the injection method and higher than 5 s for the dipping method to determine the time-response of chemosensors. This is sufficient to investigate the time-response of most optical sensors.

The dynamic characteristics of the optical pH sensor based on a polysiloxane−polyethylene glycol composite polymer with a pH responsive triangulenium dye reveal that the sensor has a response time of t_{90} = 71 ± 12 s when the pH is increased, and that the response varies with the magnitude of the activity step when the pH is decreased (average t_{90} = 22 ± 5 s). The difference was rationalized using two models for the mass transport of protons. The models differ in the type of rate limiting mass transport: For the pH increase, the response time is limited by diffusion of protons within the sensor material. For a pH decrease, the response time is determined by the thickness of the boundary layer on the optode.

We conclude that the detailed studies as the ones described here are not only necessary if we are to compare sensor performance, but also reveal important properties of the sensor chemistry and provide the information needed for informed sensor optimization.

MATERIALS AND METHODS

MES monohydrate and MES sodium salt were purchased from Sigma-Aldrich in analytical grade (>99.0%). Deionized water was used without further purification.

Preparation of Sample Solutions. All measurements were carried out in sample solutions containing 0.020 M MES buffer. Two stock solutions containing 0.020 M MES were prepared from MES monohydrate (buffer A) and MES sodium salt (buffer B), respectively. pH values of the two solutions were 4.2 and 7.8. Sample solutions containing 0.020 M MES at different pH values ranging from pH 4.2 to 7.8 were prepared by mixing buffer A and buffer B in different ratios. Sample solutions containing 0.020 M MES at pH values outside the 4.2−7.8 range were prepared from pure solutions of either buffer A or buffer B, respectively, titrated with 1 M HCl or 1 M NaOH.

Optical pH Sensor. The fabrication of sensor spots is described elsewhere.[16,17] Each sensor spot was glued to the outside tip of an injection molded polycarbonate sheath using a transparent UV-curing glue (UV adhesive U305, Cyberbond Europe GmbH), see Figure 1A. A home-built hardware setup was used in the experiments.[17] A blue-green LED (505 nm, NSPE310S, Nichia) was used as the light source. The light was filtered using a 550 nm short-pass filter (Omega Optical) before it was coupled to a QR600-7-VIS125BX optical probe (Ocean Optics). The polycarbonate sheath was placed over the optical probe centering the tip of the probe 3 mm above the sensor spot. The fluorescence light emitted from the sensor spot was collected through the QR600-7-VIS125BX optical probe (Ocean Optics) and guided into the fiber spectrometer (FREEDOM vis-NIR, Ibsen Photonics) through a 560 nm long-pass filter (Omega Optical). An automated software routine allowed a readout of 12 fluorescence spectra per minute.

pH-Meters. Two pH-meters (Mettler-Toledo Seven Compact) were used to measure pH. The pH meters were equipped with two different pH electrodes (a Mettler-Toledo, InLab Micro Pro and a Mettler-Toledo, InLab Expert Pro) both with a diameter of 5 mm and a surface area of ∼40 mm^2. The pH electrodes were calibrated using a series of four standard technical buffer solutions at pH 2.00, 4.01, 7.00, and 10.00 (NIST traceable, Mettler-Toledo, InLab solutions).

Recording Time-Response Curves Using the Injection Method. The experimental setup is shown in Figure 1B. A bar magnet (length 30 mm, 6 mm Ø) was placed in a 450 mL crystallization bowl (115 mm Ø, height 65 mm), hereafter denoted as the reservoir. Then, 250 mL sample solution was transferred to the reservoir creating a liquid column with a height of 27 mm. The reservoir was placed on a magnetic stirrer, and agitation at 500 rpm was applied unless otherwise stated. A black table was placed above the reservoir to shield the sample solution from changes in ambient light. pH electrodes and optodes were immersed into the reservoir through the black table 40 mm from the vortex centre with an angle of 90° with respect to the liquid surface and positioned with the tip 10 mm beneath the surface. The electrodes and optodes were allowed to pre-equilibrate for 10 min.

Recording time-response curves of optodes: After pre-equilibration, data were recorded for at least 3 min before an aliquot of either 1 M HCl or 1 M NaOH was injected. A small volume of HCl or NaOH was injected from a 20 mL syringe equipped with Teflon tubing (0.5 mm Ø), 40 mm from the vortex centre and 1 cm below the surface of the sample solution using a syringe pump (KDS, Legato 100) with a speed of 30 mL/min, see the Supporting Information for details. Maximum injection duration was 8 s. The temperature was recorded simultaneously using the pH meters. The temperature was constant within 0.2 °C throughout each experiment. Optical signals were read out every 5 s ($t_{res,O}$ = 5 s). The experiment was stopped after recording data for at least 5 times t_{90}.

Recording time-response curves of electrodes: After pre-equilibration, data were recorded for at least 1.5 min before an aliquot of either 1 M HCl or 1 M NaOH was injected from a 50 mL syringe equipped with Teflon tubing (0.5 mm Ø). HCl/NaOH was injected through an inlet tube at the solution surface, see the Supporting Information for details. The inlet tube was positioned 20 mm from the vortex centre with an opening (5 mm Ø) at the bottom of the reservoir. Injection was performed using a syringe pump (KDS, Legato 100) with a speed of 100 mL/min. Maximum injection duration was 2.4 s. The temperature was recorded simultaneously with the electric potential on the pH meters. The temperature was constant within 0.2 °C throughout each experiment. Optical signals were read out every second ($t_{res,E}$ = 1 s). The experiment was stopped after recording data for at least 5 times t_{90}.

Recording the Response Using the Dipping Method. The experimental setup is shown in Figure 1C. Two sample solutions consisting of 0.02 M MES buffer with different pH values corresponding to the activity step change were prepared: A bar magnet (length 20 mm, 6 mm Ø) was placed in a crystallization bowl (95 mm Ø, height 55 mm), hereafter denoted the reservoir. Then, 200 mL sample solution was transferred to the reservoir creating a liquid column with a height of 30 mm. Two reservoirs were placed on magnetic

DOI: 10.1021/acsomega.9b00795
ACS Omega 2019, 4, 8381−8389

stirrers, and agitation at 500 rpm was applied (IKA C-Mag HS7). A black table was placed above the reservoir to shield the sample solution from changes in ambient light that may interfere with the optical signals. pH electrodes and optodes (as described above) were immersed into the reservoir through the black table 20 mm from the vortex centre with an angle of 90° with respect to the liquid surface and positioned with the tip 15 mm beneath the surface. The electrodes and optodes were allowed to pre-equilibrate for 10 min in the first buffer solution. Hereafter, data were recorded for at least 3 min before the sensors were rapidly removed from the first buffer solution and immediately immersed into the second buffer solution. This procedure did not take more than 3 s. The temperature was recorded using the pH meters, and was constant within 0.1 °C throughout the experiment. Electric potentials were read out every second ($t_{res,E}$ = 1 s) and optical signals were read out every 5 s ($t_{res,O}$ = 5 s). The experiment was stopped after recording data for at least 5 × t_{90}.

■ ASSOCIATED CONTENT

Supporting Information

The Supporting Information is available free of charge on the ACS Publications website at DOI: 10.1021/acsomega.9b00795.

Detailed experimental descriptions, all data recorded in the form of time-response curves, and fitted time-response data (PDF)

■ AUTHOR INFORMATION

Corresponding Authors

*E-mail: Christian@chem.ku.dk (C.G.F.).
*E-mail: TJS@chem.ku.dk (T.J.S.).

ORCID

Thomas J. Sørensen: 0000-0003-1491-5116

Notes

The authors declare the following competing financial interest(s): TJS is a founder and current owners of FRS-systems ApS, a University of Copenhagen Spin-Out company commercializing the optical pH sensors investigated in this manuscript.

■ ACKNOWLEDGMENTS

The authors thank Villum Fonden (grant#14922), BIOPRO, Innovationsfonden (grant#5179-00914B), UpX, and the University of Copenhagen.

■ ABBREVIATIONS

APTES, (3-aminopropyl)triethoxysilane; DAOTA, diazaoxatriangulenium; DO, dissolved oxygen; ETES, ethyltriethoxysilane; GPTMS, (3-glycidyloxypropyl)trimethoxysilane; HPTS, 8-hydroxypyrene-1,3,6-trisulfonic acid; IUPAC, International Union of Pure and Applied Chemistry; LED, light emitting diode; MES, 2-(*N*-morpholino)ethanesulfonic acid; MTMOS, methyltrimethoxysilane; PDMS, polydimethylsiloxane; PET, polyethylene terephthalate; PMMA, poly(methyl methacrylate); PrTES, propyltriethoxysilane; PhTES, phenyltriethoxysilane; PS, polystyrene; TDI, terrylene diimide; TEOS, tetraethylorthosilicate; TMOS, tetramethylorthosilicate

■ REFERENCES

(1) Sørensen, S. P. L. Über die Messung und die Bedeutung der Wasserstoffionenkonzentration bei enzymatischen Prozessen. *Biochem. Z.* **1909**, *21*, 131−304.
(2) Cremer, M. Über die Ursache der elektromotorischen Eigenschaften der Gewebe, zugleich ein Beitrag zur Lehre von den polyphasischen Elektrolytketten. *Z. Biol.* **1906**, *47*, 562−608.
(3) Haber, F.; Hlemensiewicz, Z. Über elektrische Phasengrenzekräfte. *Z. Phys. Chem.* **1909**, *67*, 385.
(4) Scholz, F. From the Leiden jar to the discovery of the glass electrode by Max Cremer. *J. Solid State Electrochem.* **2011**, *15*, 5−14.
(5) Belyustin, A. A. The centenary of glass electrode: from Max Cremer to F. G. K. Baucke. *J. Solid State Electrochem.* **2011**, *15*, 47−65.
(6) Gotor, R.; Ashokkumar, P.; Hecht, M.; Keil, K.; Rurack, K. Optical pH Sensor Covering the Range from pH 0-14 Compatible with Mobile-Device Readout and Based on a Set of Rationally Designed Indicator Dyes. *Anal. Chem.* **2017**, *89*, 8437−8444.
(7) Bender, M.; Bojanowski, N. M.; Seehafer, K.; Bunz, U. H. F. Immobilized Poly(aryleneethynylene) pH Strips Discriminate Different Brands of Cola. *Chem.—Eur. J.* **2018**, *24*, 13102−13105.
(8) Weidgans, O. S. W. a. B. M., Fiber optic chemical sensors and biosensors: a view back. In *Optical Chemical Sensors*; Baldini, F.; Chester, A. N.; Homola, J.; Martellucci, S., Eds.; Springer, 2004; pp 17−46.
(9) Wencel, D.; Abel, T.; McDonagh, C. Optical chemical pH sensors. *Anal. Chem.* **2014**, *86*, 15−29.
(10) Lin, J. Recent development and applications of optical and fiber-optic pH sensors. *TrAC, Trends Anal. Chem.* **2000**, *19*, 541−552.
(11) Wolfbeis, O. S. Editorial: Probes, Sensors, and Labels: Why is Real Progress Slow? *Angew. Chem., Int. Ed.* **2013**, *52*, 9864−9865.
(12) Card, C.; Clark, K.; Furey, J. Adoption of Single-Use Sensors for BioProcess Operations. *BioProcess Int.* **2011**, *9*, 36−42.
(13) Weichert, H.; Lüders, J.; Becker, M.; Adams, T.; Weyand, J. Integrated Optical Single-Use Sensors: Moving Toward a True Single-Use Factory for Biologics and Vaccine Production. *BioProcess Int.* **2014**, *12*, 20−24.
(14) Janzen, N. H.; Schmidt, M.; Krause, C.; Weuster-Botz, D. Evaluation of fluorimetric pH sensors for bioprocess monitoring at low pH. *Bioprocess Biosyst. Eng.* **2015**, *38*, 1685−1692.
(15) Diehl, B. H.; La Pack, M. A.; Wang, T. Y.; Kottmeier, R. E.; Kaneshiro, S. M.; Brandenstein, M. C.; Zhang, Y. C.; Chiu, Y. C.; Yoon, S.; Saucedo, V. M. A Biopharmaceutical Industry Perspective on Single-Use Sensors for Biological Process Applications. *BioPharm Int.* **2015**, *28*, 28−31.
(16) Frankær, C. G.; Hussain, K. J.; Rosenberg, M.; Jensen, A.; Laursen, B. W.; Sørensen, T. J. A Biocompatible Microporous Organically Modified Silicate Material with Rapid Internal Diffusion of Protons. *ACS Sens.* **2018**, *3*, 692.
(17) Frankær, C. G.; Hussain, K. J.; Dörge, T. C.; Sørensen, T. J. Optical Chemical Sensor Using Intensity Ratiometric Fluorescence Signals for Fast and Reliable pH Determination. *ACS Sens.* **2019**, *4*, 26−31.
(18) Irving, H. M.; Zettler, H.; Baudin, G.; Preiser, H.; Guilbault, G. G.; Menis, O.; Rice, N. M.; Robertson, A. J. B.; Docherty, A. C.; Fischer, W.; Kaiser, H.; Kirkbright, G. F.; Samuelson, O.; Svehla, G. G.; Tölg, G.; West, T. S.; Tawfik, H. A. Recommendations for Nomenclature of Ion-Selective Electrodes. *Pure Appl. Chem.* **1976**, *48*, 127−132.
(19) Lindner, E.; Tóth, K.; Pungor, E. Definition and Determination of Response-Time of Ion-Selective Electrodes. *Pure Appl. Chem.* **1986**, *58*, 469−479.
(20) Buck, R. P.; Lindner, E. Recomendations for nomenclature of ion-selective electrodes. *Pure Appl. Chem.* **1994**, *66*, 2527−2536.
(21) Sydenham, P. H., Static and Dynamic Characteristics of Instrumentation. In *The Measurement Instrumentation and Sensors Handbook*, Webster, J. G., Ed.; CRC Press, 1998.
(22) Kalantar-zadeh, K., *Sensors An Introductory Course*; Springer, 2013.

DOI: 10.1021/acsomega.9b00795
ACS Omega 2019, 4, 8381−8389

(23) Frankær, C. G.; Sørensen, T. J. A Unified Approach for Investigating Chemosensor Properties – Dynamic Characteristics. *Analyst* **2019**, *144*, 2208.
(24) Maccà, C. Response time of ion-selective electrodes. *Anal. Chim. Acta* **2004**, *512*, 183–190.
(25) Morf, W. E.; Lindner, E.; Simon, W. Theoretical Treatment of Dynamic-Response of Ion-Selective Membrane Electrodes. *Anal. Chem.* **1975**, *47*, 1596–1601.
(26) Laursen, B. W.; Krebs, F. C. Synthesis of a triazatriangulenium salt. *Angew. Chem.* **2000**, *39*, 3432–3434.
(27) Laursen, B. W.; Krebs, F. C. Synthesis, structure, and properties of azatriangulenium salts. *Chem.–Eur. J.* **2001**, *7*, 1773–1783.
(28) Frankær, C. G.; Rosenberg, M.; Santella, M.; Hussain, K. J.; Laursen, B. W.; Sørensen, T. J. Tuning the pKa of a pH Responsive Fluorophore and the Conse-quences for Calibration of Optical Sensors based on a Single Fluorophore but Multiple Receptors. *ACS Sens.* **2019**, *4*, 764.
(29) Rosenberg, M.; Laursen, B. W.; Frankær, C. G.; Sørensen, T. J. A Fluorescence Intensity Ratiometric Fiber Optics–Based Chemical Sensor for Monitoring pH. *Adv. Mater. Technol.* **2018**, *3*, 1800205.
(30) Sørensen, T. J.; Rosenberg, M.; Frankær, C. G.; Laursen, B. W. An Optical pH Sensor Based on Diazaoxatriangulenium and Isopropyl-Bridged Diazatriangulenium Covalently Bound in a Composite Sol–Gel. *Adv. Mater. Technol.* **2018**, *4*, 1800561.
(31) Wolfbeis, O. S. Fiber-Optic Chemical Sensors and Biosensors. *Anal. Chem.* **2008**, *80*, 4269–4283.
(32) Fleet, B.; Ryan, T. H.; Brand, M. J. D. Investigation of Factors Affecting Response-Time of a Calcium Selective Liquid Membrane Electrode. *Anal. Chem.* **1974**, *46*, 12–15.
(33) Karlberg, B. Ion-Exchange Properties of Gel Layer of Some Hydrogen-Ion-Selective Glass Electrodes. *J. Electroanal. Chem.* **1973**, *45*, 127–139.
(34) Tóth, K.; Stulík, K.; Kutner, W.; Fehér, Z.; Lindner, E. Electrochemical detection in liquid flow analytical techniques: Characterization and classification - (IUPAC Technical Report). *Pure Appl. Chem.* **2004**, *76*, 1119–1138.
(35) Lindner, E.; Toth, K.; Pungor, E. Response-Time Curves of Ion-Selective Electrodes. *Anal. Chem.* **1976**, *48*, 1071–1078.
(36) Tóth, K.; Gavallér, I.; Pungor, E. Transient Phenomena of Ion-Selective Membrane Electrodes. *Anal. Chim. Acta* **1971**, *57*, 131–135.
(37) Rovati, L.; Fabbri, P.; Ferrari, L.; Pilati, F. Construction and evaluation of a disposable pH sensor based on a large core plastic optical fiber. *Rev. Sci. Instrum.* **2011**, *82*, 023106.
(38) Kosch, U.; Klimant, I.; Werner, T.; Wolfbeis, O. S. Strategies to design pH optodes with luminescence decay times in the microsecond time regime. *Anal. Chem.* **1998**, *70*, 3892–3897.
(39) Nivens, D.; Schiza, M. V.; Angel, S. M. Multilayer sol-gel membranes for optical sensing applications: single layer pH and dual layer CO2 and NH3 sensors. *Talanta* **2002**, *58*, 543–550.
(40) Wang, E.; Chow, K.-F.; Kwan, V.; Chin, T.; Wong, C.; Bocarsly, A. Fast and long term optical sensors for pH based on sol-gels. *Anal. Chim. Acta* **2003**, *495*, 45–50.
(41) Lee, S. T.; Gin, J.; Nampoori, V. P. N.; Vallabhan, C. P. G.; Unnikrishnan, N. V.; Radhakrishnan, P. A sensitive fibre optic pH sensor using multiple sol-gel coatings. *J. Opt. A: Pure Appl. Opt.* **2001**, *3*, 355–359.
(42) Rayss, J.; Sudolski, G. Ion adsorption in the porous sol-gel silica layer in the fibre optic pH sensor. *Sens. Actuators, B* **2002**, *87*, 397–405.
(43) Sánchez-Barragán, I.; Costa-Fernández, J. M.; Sanz-Medel, A.; Valledor, M.; Ferrero, F. J.; Campo, J. C. A ratiometric approach for pH optosensing with a single fluorophore indicator. *Anal. Chim. Acta* **2006**, *562*, 197–203.
(44) Kocincova, A. S.; Borisov, S. M.; Krause, C.; Wolfbeis, O. S. Fiber-optic microsensors for simultaneous sensing of oxygen and pH, and of oxygen and temperature. *Anal. Chem.* **2007**, *79*, 8486–8493.
(45) Han, C.; Yao, L.; Xu, D.; Xie, X. C.; Zhang, C. S. High-resolution Imaging of pH in Alkaline Sediments and Water Based on a New Rapid Response Fluorescent Planar Optode. *Sci. Rep.* **2016**, *6*, 26417.
(46) Gonçalves, H. M. R.; Maule, C. D.; Jorge, P. A. S.; Esteves da Silva, J. C. G. Fiber optic lifetime pH sensing based on ruthenium(II) complexes with dicarboxybipyridine. *Anal. Chim. Acta* **2008**, *626*, 62–70.
(47) Wencel, D.; MacCraith, B. D.; McDonagh, C. High performance optical ratiometric sol–gel-based pH sensor. *Sens. Actuators, B* **2009**, *139*, 208–213.
(48) Wencel, D.; Barczak, M.; Borowski, P.; McDonagh, C. The development and characterisation of novel hybrid sol–gel-derived films for optical pH sensing. *J. Mater. Chem.* **2012**, *22*, 11720.
(49) Jurmanović, S.; Kordić, Š.; Steinberg, M. D.; Steinberg, I. M. Organically modified silicate thin films doped with colourimetric pH indicators methyl red and bromocresol green as pH responsive sol-gel hybrid materials. *Thin Solid Films* **2010**, *518*, 2234–2240.
(50) Lobnik, A.; Oehme, I.; Murkovic, I.; Wolfbeis, O. S. pH optical sensors based on sol-gels: Chemical doping versus covalent immobilization. *Anal. Chim. Acta* **1998**, *367*, 159–165.
(51) Cajlakovic, M.; Lobnik, A.; Werner, T. Stability of new optical pH sensing material based on cross-linked poly(vinyl alcohol) copolymer. *Anal. Chim. Acta* **2002**, *455*, 207–213.
(52) Lindner, E.; Toth, K.; Pungor, E.; Berube, T. R.; Buck, R. P. Switched Wall Jet for Dynamic-Response Measurements. *Anal. Chem.* **1987**, *59*, 2213–2216.
(53) Rangarajan, R.; Rechnitz, G. A. Dynamic-Response of Ion-Selective Membrane Electrodes. *Anal. Chem.* **1975**, *47*, 324–326.
(54) Bakker, E.; Bühlmann, P.; Pretsch, E. Carrier-based ion-selective electrodes and bulk optodes. 1. General characteristics. *Chem. Rev.* **1997**, *97*, 3083–3132.

DOI: 10.1021/acsomega.9b00795
ACS Omega 2019, 4, 8381–8389